BIBECHANA
ISSN 2091-0762 (Print), 2382-5340 (Online)
Journal homepage: http://nepjol.info/index.php/BIBECHANA
Publisher: Department of Physics, Mahendra Morang A.M. Campus, TU, Biratnagar, Nepal

Substitutional Sodium Doping on Tungsten Ditelluride: A First-principles Study

Bibek Subedi and Narayan Prasad Adhikari*
Central Department of Physics Tribhuvan University Kirtipur Kathmandu Nepal

*Email: narayan.adhikari@cdp.tu.edu.np;vivek13.bs@gmail.com

Article Information:
Received: January 08, 2022
Accepted: July 10, 2022

Keywords:
First-principles calculationsElectronic structures
Tungsten Ditelluride
Sodium atom doping

ABSTRACT

For the investigation of structural, electronic and magnetic properties of pure and single sodium atom doped tungsten ditelluride monolayer, first-principles calculations based on density functional theory (DFT) have been used. As the band gaps are on the order of the solar spectrum, they are commonly utilized in photovoltaic and opto-electronic systems. Although WTe_2 has a wide range of technological applications in photo electrochemical cells and semiconductors, there are few theoretical and practical research on electronic structure calculations. To explore the band gap and other electronic and magnetic characteristics, we doped a single Na atom into WTe_2 system. The substrate has two possible sites for sodium doping, one tungsten site (Na_W) and the other tellurium site (Na_{Te}). On doping sodium atom at the tellurium site of 3×3 supercell, it seems to have metallic behaviour while the pristine form was semiconductor. The formation energies for both site doping have been estimated which predict that tellurium site doping is more preferable with lower formation energy. The Te site is magnetic in nature, according to density of states (DOS) estimates, with a somewhat unsymmetric DOS plot. For tellurium site total magnetization is about $0.93\mu_B$ while the pristine form was non-magnetic. The magnetism arises due to the redistribution of charge density as a result of adding a sodium atom as an impurity.

DOI: https://doi.org/10.3126/bibechana.v19i1-2.46429

1. Introduction

Two-dimensional (2D) materials are crystalline materials made up of single layers of atoms having thickness in the range of few nanometers or less. The importance of 2D materials has been found in electrodes, photovoltaics, and semiconductors, among

other applications. These are ultrathin nanomaterials with substantial anisotropy and chemical functionality. [1]. They vary greatly in form, size, biocompatibility and degradability, as well as optical, mechanical, and chemical characteristics [2]. Graphene, a single sheet of graphite, was dis-covered in 2004 and became the first known 2D substance. Many more 2D materials, such as transition metal dichalcogenides (TMDC) and hexagonal boron nitrides (h-BN), were discovered after graphene. The TMDC materials follow MX_2 structure, where M is a IVB-VIB (IVB - Ti & Zr, VB - Nb & Ta, VIB - Mo & W) transition metal and X is a chalcogen atom (S, Se, Te). According to the nature of the combination of transition metal and chalcogen, the resulting material can vary its properties from semiconducting to metallic and even superconducting state. Also, if the bulk crystal is reduced to fewer layers, the band structure of many TMDCs changes distinctively, resulting in a unique sensitivity of TMDC properties to thickness [3].

In the bulk form, the crystal of 2H-WTe_2 crystallize in the hexagonal structure belonging to the space group $P6_3/mmc$ which corresponds to the space group number 194. The crystal structure of WTe_2 are composed of van der Walls-bonded Te-W-Te units. These stable units are WTe_2 monolayers, which contains two hexagonal planes of Te atoms and an intermediate plane of W atom. There exists ionic-covalent interaction between these hexagonal planes in which the chalcogen atoms are (Te) are arranged in trigonal prismatic structure [4].

In the monolayer of WTe_2, the W atom is trapped between two W atoms, which has a honeycomb structure. In WTe_2 structure, the bond length between two W atoms and W & Te atoms are found to be 3.51 Å and 2.73 Å respectively. The W-Te-W atoms forms the relaxed bond angle of 80.27º [5]. The band structure calculation of 2H- WTe_2 along the high symmetry points Γ-M-K-Γ shows the indirect band gap of 0.81 eV with valance band maxima at Γ-points and conduction band minima at between Γ and K points. However, in 1H- WTe_2, at high symmetry point K, direct band gap of 1.18 eV was observed. So, when the bulk structure is replaced by a single layer, the band gap switches from indirect to direct [4]. Among the various properties, WTe_2 exhibit interesting properties like quantum spin Hall effect and extremely large non saturating magnetoresistance in the monolayer limit [6]. The origin of large magnetoresistance is due the perfect balance between holes and electrons, which are sensitive to external pressure [7]. WTe_2 exhibit quantum transport properties, which includes superconductivity observed in the bulk crystal at high pressure [8], in multilayer flakes by proximity [9], and in monolayer by gating [10,11]. Furthermore, it shows quantum spin Hall effect up to 100 K in monolayer limit and Type-II Weyl semi-metallic band structure[6]. Despite the fact that WTe_2 is not a common material like all transition metal tellurides, it is briefly discussed as a member of this sub-family of TMDC due to its peculiar features, which have made it a possibility for enormous magnetoresistance and superconductivity.

Many theoretical and experimental works have been done on electronic and magnetic properties of WTe_2. The electronic band structure and density of states of pristine form is studied theoretically and experimentally. The change in band structure and other properties after the doping of the elements like H, Li, Be have been studied earlier. So, we are going to study the change in properties of pristine form after doping of Na atom. By substituting a tungsten or a tellurium atom of pure tungsten ditelluride with a sodium atom, doping can be done. This might bring about changes in the electronic and magnetic behavior which may help keep a pace further ahead in this research eld.

E. Igmubor *et al.*, in 2017 studied the doping of H, Li and Be on monolayer WTe_2. They found the formation energies of X dopant substituted for W between 3.59 and 2.61 eV. In their study, they found that Li_W

defect having formation energy of 2.14 eV was the most favorable. Also, it was known that H_W induced no magnetic moment while Li_W and Be_W induced magnetic moment of 3.44 and 0.05 μ_B respectively [5].

The element we want to dope in our system, Sodium ([Ne] $3s^1$) is soft, silvery white metal belonging to group I of the periodic table. The Sodium atom has body-centered cubic crystal structure and it is paramagnetic in nature. Due to the single valance electron, sodium is a good conductor of heat and electricity and is also highly reactive in nature. Thus, by using substitutional doping, the sodium metal atom should fit readily into the WTe_2 sheet. In our work, we apply spin polarized density functional theory (DFT) method to investigate the impact and variation in the electronic and magnetic properties of Na doped WTe_2 nanosheet compared with pure WTe_2. Following this section, we go over the computational techniques, findings and discussion and conclusions in that sequence.

2.Methods and computational details

We used the Quantum ESPRESSO code to conduct first principles calculations to examine the stability, electronic and magnetic properties of pristine and sodium doped Tungsten Ditelluride in the context of density functional theory with van der Waals (vdW) interactions [12-14]. The generalized gradient approximation (GGA) created by three scientists Perdew, Burke, and Ernzerhof (PBE) [15] was employed to include the electronic exchange and correlation impact in our system. We used the Kresse-Joubert (KJ) projector augmented wave (PAW) pseudopotential to replace the complex effects of non-valance (*i.e.*, core) electrons and nucleus with an equivalent potential as a result only active valance electrons are explicitly included throughout our calculation.

To avoid any chance of contact from adjoining layers of WTe_2, a vacuum of 20 Å was made in the perpendicular direction to the plane of the WTe_2 mono-layer (z-axis). The geometrically optimized structure was obtained by allowing our structure to relax under Broyden-Fletcher-Goldfarb-Shanno (BFGS) [16] scheme until the change in total energy was less than 10^{-4} Ry between two successive self-consistent field (scf) steps while each component of force acting is less than 10^{-3} Ry/Bohrs. Following the relaxation calculations, we calculated self-consistent total energy. The Brillouin zone of WTe_2 was obtained in K-space adopting Monkhorst-Pack technique [17] with an estimated value of mesh of K-points derived from the convergence test. We utilized a K-point mesh of 10×10×1 for relaxation calculation and a K-point mesh of 14×14×1 for all other computation. We picked the wave function cutoff energy value of 50 Ry and the charge density cutoff energy value of 500 Ry using the convergence test. Optimization calculation of lattice parameter was done before the relaxation calculation and the optimized value of lattice parameter was obtained as 6.715 Bohr. We have also utilized 'Marzarri-Vanderbilt (m-v)' [18] technique of smearing or cold smearing with 0.01 Ry smearing width. In addition, for self-consistency, we used the 'david' diagonalization technique with 'plain' mixing mode and 0.7 mixing factor.

3. Results and Discussion

In this section, we discuss about the results of calculations as well as analyze the results and interpret it. The main goal of our work is to investigate the electronic and magnetic characteristics of pristine and sodium doped tungsten ditelluride using Density Functional Theory (DFT) simulating under Quantum ESPRESSO (QE). Band structure, density of states (DOS), and projected density of states (PDOS) computations were used to explain the electronic and magnetic features of pristine and Na doped 3×3×1 supercell of WTe_2.

A. Structure and formation energy

By taking optimized values of ecutwfc, k-points and the lattice parameter, we defined our system in the PWscf input file. Taking the help of XCrySDen, we first obtained the

primitive cell structure, figure(1), and then the 3×3 supercell, figure (2) using this input file. Both of the primitive cell and supercell were allowed to relax using BFGS quasi-newton algorithm for structural relaxation.

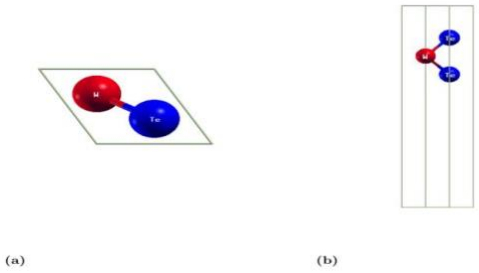

(a) (b)

FIG. 1 (a) Top view (b) side view of WTe_2 primitive cell

There was very slight change in the atomic position after relaxation. The corresponding bond lengths and bond angles were also changed by small amount in the primitive cell as shown in table (I).

TABLE I. Optimized structural parameters of the relaxed primitive WTe_2 cell

Primitive cell (3 atoms)	Lattice parameter	a=b=3.554Å, c=20Å
	W-Te bond length	2.739Å
	Te-W-Te bond length	83.010º

The parameters of our investigation are in great agreement with previously investigated values, as shown in table (I). In the study of E. Igumbor *et al*., the value of bond length between W-W and W-Te atoms was found to be 3.51 Å and 2.73 Å respectively [5]. Also, our values of bond length agree with that of E. Torun *et al*., which are: 3.55 Å and 2.73 Å for W-W and W-Te respectively [19].

The input file for 3×3 supercell of tungsten ditelluride was constructed and then the system was allowed to relax. It is a unit cell with 27 atom basis and size of cell three times that of primitive cell.

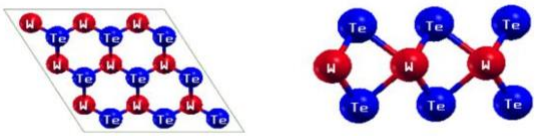

(a) (b)

FIG. 2 (a) Top view (b) side view of 3×3 supercell of WTe_2 monolayer

The structural parameters of this supercell were calculated and presented in table (II).

TABLE II. Optimized structural parameters of the relaxed 3x3 WTe_2 monolayer

3×3 Supercell (27 atoms)	Unit cell size	a=b=10.661A, c=20Å
	W-Te bond lengths	2.739Å, 2.739Å, 2.739Å
	W-W bond length	3.553Å, 3.553Å, 3.553Å
	W-Te-W bond angles	80.863º

The supercell structure shows the replication of atoms in x and y direction. The bond length and bond angles for particular atoms were also equal so the system can be said to be perfectly symmetric and homogeneous.

The doping of Na on the pure system produces several distortions. Nearest W atoms

(in Na_{Te}) and nearest Te atoms (in Na) are drawn away from the plane. As a result, the bond lengths and angles of the nearest neighbor W-Te are likewise changed. The deformed structure of the system following Na doping may be seen in figures (3) and (4).

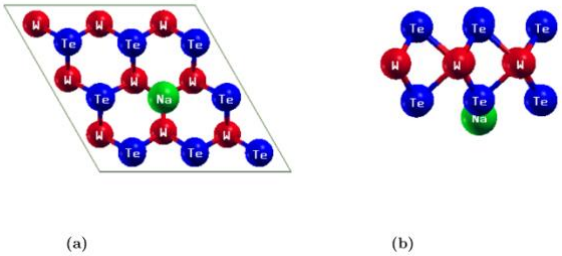

FIG. 3 (a) Top view (b) Side view of Na substituted WTe_2 at Te site (Na_{Te})

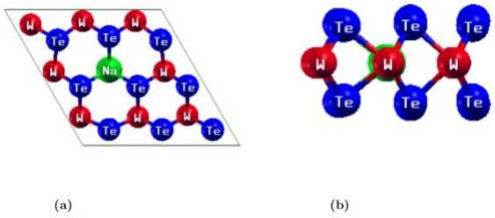

FIG. 4 (a) Top view (b) side view of Na substituted WTe_2 at W site (Na_W)

The structural parameters of the distorted system after Na doping are presented in table (III) and (IV).

TABLE III. Structural characteristics of WTe_2 sheet with Na atom doping at Te site (Na_{Te})

W-Na-W bond angles	59.486º, 59.486º	59.486º,
W-Na bond length	3.282Å, 3.282Å	3.282Å,
Nearest neighbor Te-W-Te bond angles	81.231º, 81.231º	81.231º,
Nearest neighbor W-Te bond lengths	2.771Å, 2.771Å	2.771Å,

TABLE IV. Structural characteristics of WTe_2 sheet with Na atom doping at W site (Na_W)

Te-Na-Te bond angles	77.967º, 77.967º	77.967º,
Te-Na bond length	2.899Å, 2.899Å	2.899Å,
Nearest neighbor W-Te-W bond angles	80.841º, 80.841º	80.841º,
Nearest neighbor Te-W bond lengths	2.799Å, 2.799Å	2.799Å,

Tables (III) and (IV) shows that in both Na_{Te} and Na_W system, the Na atom has been repelled from the buckled plane. There occur significant increase of W-Na and Te-Na bond length (3.282 Å and2.899 Å) than W-Te bond length (2.739 Å) in pristine form. As seen in the above tables (III) and (IV), the nearest neighbor bond lengths and bond angles surrounding the doping site have been modified by a little amount. Beyond this, we discovered structural changes in the whole sheet, with the degree of distortion decreasing as we go away from the doped atom.

The stability of doped system was investigated by calculating the defect formation energy. The defect formation energy (E_F) [20] can be calculated by formula:

$$E_F = (E_{Na} - E_P) - (E_1 - E_2)$$

Where, E_{Na} represents the total energy of Na doped WTe_2, E_P represents the total energy of pure WTe_2, E_1 represents the energy of single Na atom and E_2 represents energy of single W or Te atom. By studying an isolated system of single atoms, the energy of isolated Na, W and Te atoms were determined using DFT with suitable pseudopotentials.

TABLE V. Calculation of formation energy using different energy values (in Rydbergs; 1 Ry = 13.6 eV)

Formation energy of Na doped WTe_2 at Te site

Study in system	Energy (Ry)
Na doped WTe_2 (E_{Na})	-13115.874
Pristine 3×3 WTe_2 (E_p)	-13369.374
Isolated Na atom(E_1)	-109.167
Isolated Te atom(E_2)	-362.429
Formation Energy (E_F)	0.238

Formation energy of Na doped WTe_2 at W site

Study in system	Energy (Ry)
Na doped WTe_2 (E_{Na})	-12718.187
Pristine 3×3 WTe_2 (E_p)	-13369.374
Isolated Na atom(E_1)	-109.167
Isolated W atom(E_2)	-759.641
Formation Energy (E_F)	0.713

The formation energy is less when Na is doped at Te site rather than at W site. Thus, the doping of Na at Te site is more favorable than at W site. From the tables above, it can be seen that all of the energy of the system under investigation are negative, indicating their stability. Both doped systems, however, have positive formation energies. It suggests, that amount of external energy should be given to con-struct the doped system, demonstrating its unstable character.

B. Electronic and Magnetic properties of pristine WTe_2

Band structure along with density of states of a quantum system is signature for the electronic properties of the material. The solution for the entire solid can be described by their nature in a single Brillouin zone. The first Brillouin zone of WTe_2 hexagonal lattice system with high symmetric points Γ-M-K-Γ is presented in figure (5). We plotted a highly fine and visible band structure plot using 100 k-points in this path.

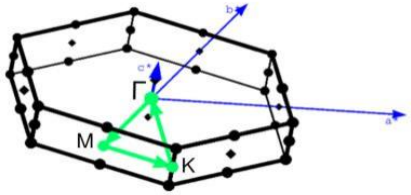

FIG. 5. First Brillouin zone of WTe_2 hexagonal lattice with Γ-M-K-Γ high symmetric points.

1. *Electronic band structure of pristine WTe_2*

In our study, band structure of pure WTe_2 single cell is calculated by taking the closed path Γ-M-K-Γ in an irreducible Brillouin zone by choosing 100 k-points grid. Figure (6) represents the band structure of pure WTe_2 unit cell with X-axis representing the high symmetric points and Y-axis representing the associated energy values. The plot shows that pristine WTe_2 is a wide gap material having a direct band gap at K-point. From our calculation, we observed that band gap is approximately 1.071 eV with valance band maximum and conduction band minimum at K-point. The value of our observation corresponds with direct band gap of 1.18 eV as calculated by A. Kumar and P.K. Ahluwalia [4]. This band gap value of 1.071 eV for primitive cell of WTe_2 signifies that the system is semiconductor. As well as we observed spin polarized calculations on 3×3 WTe_2 supercell and obtained the band structures for up-spin and down-spin electrons.

The band structures calculation shows that the arrangement of Kohn-Sham states in reciprocal space is identical for both spins. The supercell of pristine WTe_2 has direct band gap at Γ-point with band gap value of 1.082 eV.

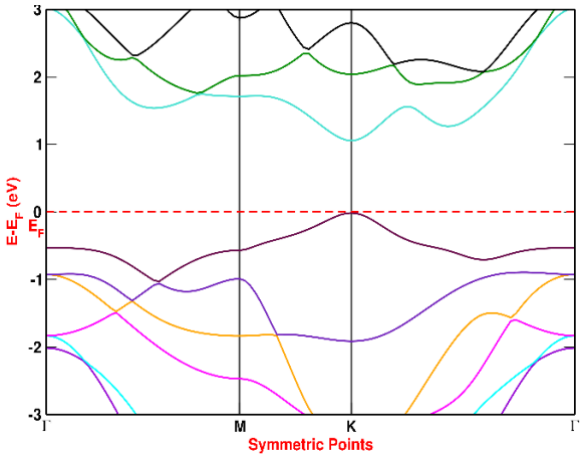

FIG. 6 Band structure of pristine WTe_2 using primitive cell, energies were calculated using the Fermi energy as a reference (E_F = 0.4962 eV).

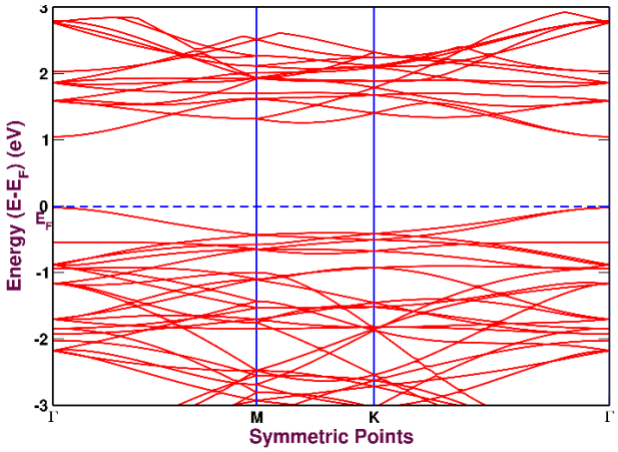

FIG.7 Band structure of pristine WTe_2 using 3×3 supercell, energies were calculated using the Fermi energy as reference (E_F=0.5053 eV).

Both primitive cell and supercell of WTe_2 shows the direct nature of the band gap. The only difference between them is that primitive cell has direct band gap at K-point while supercell has at Γ-point. The change in band structure on going from pristine to supercell is due to the band folding, as the Brillouin zone of the supercell is smaller than that of corresponding unit cell. This makes the bands of primitive cell in first Brillouin zone to get folded into supercell Brillouin zone. The supercell Brillouin zone contains large numbers of horizontal looking bands, which does not resemble the original band structure. This makes the change in the band structure on going from primitive cell to supercell, however the symmetric points remain same[21]. Band folding occurs as a result of hidden translation symmetry inside the supercell. This is because, while performing calculation on the supercell, the translational relations between unit cells within the supercell are ignored. On making larger supercell and sampling the Brillouin zone at high symmetric point, the band structure is collapsed into an energy diagram. Since there is still the translational symmetry, we can get band structure from such calculation by unfolding the band. That means, we can obtain unit cell band structure from supercell by unfolding it.

2. *Density of States (DOS) of pristine WTe_2*

The DOS plot validates the band gap argument provided by the band structure plot and also provides information on the system's magnetization. The DOS plot of 3×3 supercell is shown in the figure (8) below.

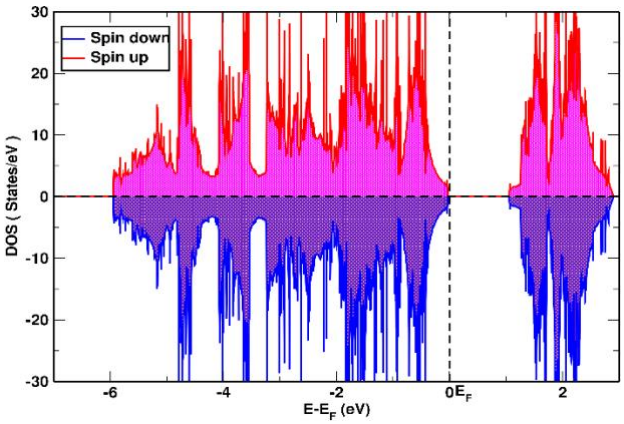

FIG. 8 Density of States for 3×3 supercell of pristine WTe_2.

From figure (8), it is clear that no spin states are available in the Fermi level. It confirms the band structure plot's conclusion that the system is semiconducting. The DOS graph demonstrates the non-magnetic character of pristine WTe_2. Our system is non-magnetic due to the symmetric distribution of accessible states for both up and down spin.

Another calculation we performed was projected density of states (PDOS) calculations for various WTe_2 orbitals. The overall DOS of the system is calculated by adding all of these orbital contributions together. The PDOS graphic shows which orbital contributes the most to the overall states of the system around the Fermi level. The PDOS plot of 3×3 supercell of pristine WTe_2 is as follows.

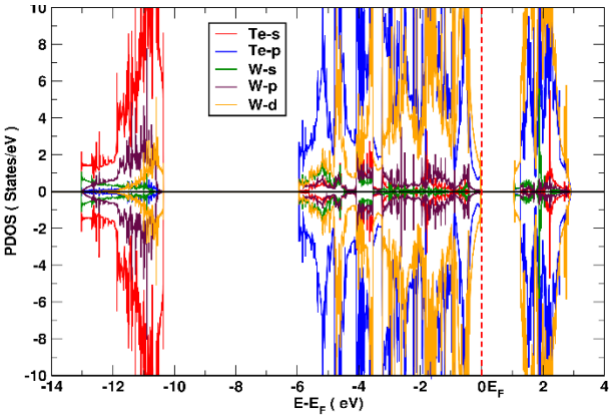

FIG. 9 PDOS for various orbitals of W and Te atoms

From this PDOS, we observed that the valence orbitals of W and Te atoms are below the Fermi level. From the figure, we observe that s & p-orbitals of Te and d-orbital of W make significant contribution, while the contribution due to the p-orbital of W is small and the contribution of s-orbital of W atom is almost absent. Furthermore, the DOS for various orbitals for both atoms in spin states up and down are perfectly symmetrical. Thus, pure WTe_2 is a nonmagnetic material and element such as Na can induce some magnetic moment on doping, which will be addressed further in the next sections.

C. Electronic and Magnetic properties of WTe_2 doped with Na atom

The inclusion of a substitutional impurity, such as Na, in the WTe_2 structure causes several modifications in its many characteristics. We also saw considerable alterations in band structure as a result of doping. On our doped system, we investigated spin polarized scf, DOS, and Projected DOS computations.

The calculation of formation energy of Na doping on two possible sites viz. W & Te and the study of stability of doping on these two sites suggests that the doping of Na at Te site is more favorable than W site. So, we present the change in the properties of pristine structure after doping of Na at Te site.

1. *Electronic band structure of Na doped WTe_2*

The band structure of Na doped WTe_2 at the Te site is shown in the diagram below. The spin polarized calculations were conducted to see the effect of doping on different spins. We observed that for up spin, electrons in the valance band crosses the Fermi level and lies 0.13 eV above the Fermi level whereas in case of down spin, no such crossover around Fermi level is found and the electrons remains in the respective valance and conduction band. These new states present are due to the effect of doping. These band structure near the Fermi level are notably different from those in pristine 3x3 WTe_2, also it is seen that energy levels of valance orbitals of W and Te are also changed around the Fermi level.

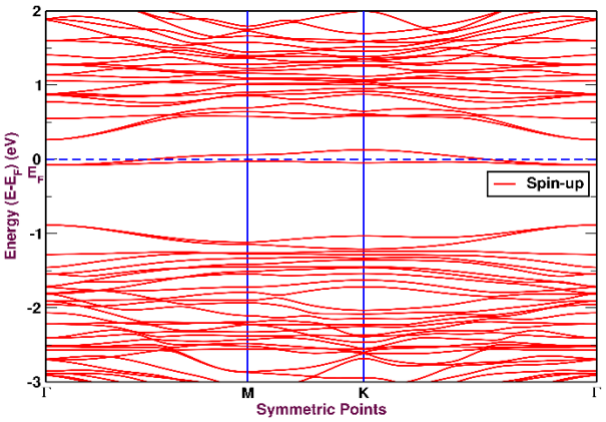

FIG. 10 Spin-up band structures of Na doped WTe_2 at Te site (Na_{Te}), Fermi level (E_f = 1.3896 eV) is fixed as zero.

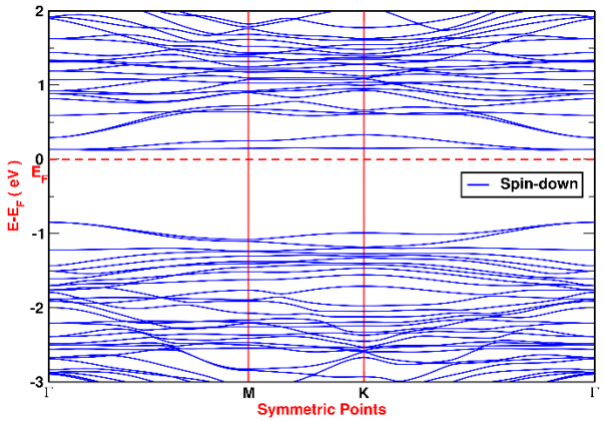

FIG. 11 Spin-down band structures of Na doped WTe_2 at Te site (Na_{Te}), Fermi level (E_f = 1.3896 eV) is fixed as zero.

The band structure diagram illustrates that doping of Na in WTe_2 sheet develop metallic character for up spin and semiconductor behavior for down spin. Furthermore, in the case of up spin, the bands from the valance band transcend the Fermi level and reach the conduction band, resulting in overlapping bands and, as a result, a metallic system. The bands stay in their respective bands without overlapping in the case of down spin, demonstrating the semiconducting nature of the material with a direct band gap of 1.007 eV at the Γ-point. The doping specially influences near about Fermi level. The Fermi energy in case of doping is 1.3896 eV, which is higher than the Fermi energy level of pristine form *i.e* 0.5053 eV. This slight increase in Fermi energy level is because of the addition of Na atom in place of Te atom.

2. *Density of States (DOS) of Na doped WTe_2*

The DOS plot of the 3×3 supercell of Na doped WTe_2 at Te site (Na_{Te}) is as follows.

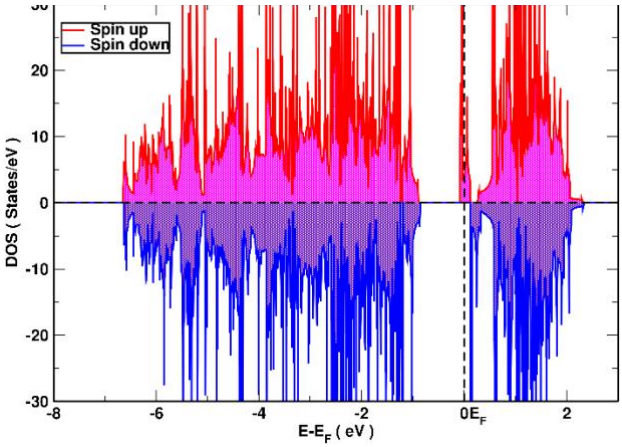

FIG. 12 Density of states plot for Na doped WTe_2 at Te site (Na_{Te})

The horizontal line in figure (12) distinguishes DOS for up-spin and down-spin, with states just above horizontal line denoting up-spin and those below the horizontal line denoting down-spin. The variation in DOS is considerable near the Fermi level. The Fermi Level line was free of any spin states in the original system. Meanwhile, the Fermi level line in a Na doped system possesses specific spin states. The Fermi level itself has been shifted up a bit in the DOS plot too, so that the system shows metallic nature in up spin state. The distribution of accessible states in case of up and down spin is asymmetrical, so that Na doped WTe_2 is magnetic. The asymmetrical nature of DOS plot gives magnetic nature to the system with total magnetization of 0.93 μ_B for Na_{Te}. The case was quite different for pristine 3×3 supercell, where up and down

DOS were symmetrical and system behaves as non-magnetic. The individual W and Te atom behave as magnetic materials as they have magnetic moment of 6 μ_B and 2 μ_B respectively.

To see more closely on the contribution of atomic orbitals of each atom we also have presented and discussed with PDOS plots as shown below.

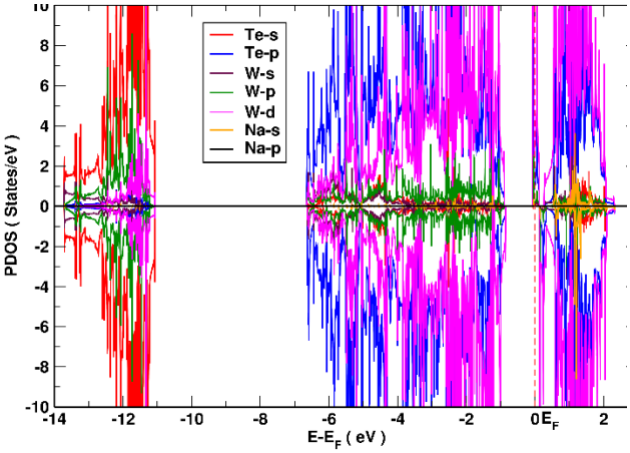

FIG.13 Projected Density of States of doped 3×3 WTe_2.

The PDOS of Na doped WTe_2 for spin states up and down is presented in figure (13) by taking fermi energy level as a reference represented by the vertical dotted lines. Spin up and spin down states are separated by the horizontal line. From the projected DOS calculations, the accessible states near Fermi level for Na doped WTe_2 at Te site, are largely because of W and Te atom. In case of W, 5d-orbital is dominant over 5p & 6s orbitals, whereas for Te, 5s & 5p-orbitals contributes significantly. Due to this the system is magnetic in nature. The contribution of 5d-orbital of W and 5s & 5p-orbitals of Te to the magnetization is relatively greater than 3s orbitals of Na. Below the Fermi level, Te-s and W-d orbitals are dominant whereas above Fermi level W-d orbitals are significant. The contribution of Na-3s orbital is almost negligible. There are large number of unoccupied vacates state below fermi level for both W and Te. The system has got magnetic nature with magnetic moment 0.93 μ_B per cell.

Conclusions and futureremarks

We conducted first principles study to look into the stability, electronic and magnetic properties of pristine and sodium doped WTe_2 system. These calculations were executed under DFT using GGA exchange correlation functional including PAW pseudo-potential implemented with Quantum ESPRESSO code.

The doping of Na atom in the system makes various distortion in the structure. The Na atom is shifted from the plane holding the W and Te atoms after doping. Regarding electronic properties we conclude that pristine WTe_2 sheet shows semi-conducting nature with a direct band gap of 1.082 eV for 3x3 supercell and direct band gap 1.071 eV for primitive cell. Both primitive and supercell shows direct nature of band gap with the difference that primitive cell has band gap at K-point while supercell has at Γ-point. This was due to the band folding while conducting calculation from unit cell to supercell. Employment of band unfolding techniques could give us more authentic results and this could be further work that can be done to enhance our knowledge about bands and band structure. The band structure of doped system was quite different from the pristine system. The doping of Na atom induces metallic character in case of up spin state with valance bands crossing the Fermi levels. However, in case of down spin state, the system shows semiconducting nature with direct band gap of 1.007 eV at Γ-point.

In case of pristine system, we found the non-magnetic nature of the system due to the symmetric structure of density of states of both spin states up and down. However, in case of doped system, the asymmetrical distribution of density of states gives the magnetic nature to the system with total magnetization of 0.93 μ_B. This magnetization

was due to the addition of Na atom in the pristine system, which caused the redistribution of charges between the doped atom and atoms of pristine system giving net magnetic moment to the system. The DOS and PDOS plot revealed that the magnetic nature of doped system is mainly due to the contribution of W-5d orbital. The contribution of 3s orbital of Na can be seen above Fermi level in small extent while below the Fermi level the its contribution is almost negligible.

Our system can be used for the potential application in the field of magnetoresistance and superconductivity. The direct-indirect gap transition shows the possible application in various fields like solar cell, electronics and photocatalysis. The current work may be advanced to investigate the charge transformation, optical, and thermal aspects of the system. Further, doping of impurities on bilayer and increasing the impurity concentration can bring new development in the study.

References

[1]X. Huang, C. Tan, Z. Yin, and H. Zhang, Advanced Materials 26 (2014) 2185.
[2]D. Nandwana and E. Ertekin, Journal of Applied Physics 117 (2015) 234304.
[3]Z. Lin, A. McCreary, N. Briggs, S. Subramanian,K. Zhang, Y. Sun, X. Li, N. J. Borys, H. Yuan, S. K. Fullerton-Shirey, *et al*., 2D Materials 3 (2016) 042001.
[4]A. Kumar and P. Ahluwalia, The European Physical Journal B 85 (2012) 1.
[5]E. Igumbor, R. E. Mapasha, and W. E. Meyer, Physica B: Condensed Matter 535 (2018)167.
[6] J. M. Woods, D. Hynek, P. Liu, M. Li, and J. J. Cha, ACS nano 13 (2019) 6455.
[7] D. Kang, Y. Zhou, W. Yi, C. Yang, J. Guo, Y. Shi, S. Zhang, Z. Wang, C. Zhang, S. Jiang, et al., Nature communications 6 (2015) 1.
[8] X.-C. Pan, X. Chen, H. Liu, Y. Feng, Z. Wei, Y.Zhou, Z. Chi, L. Pi, F. Yen, F. Song, *et al*., Nature communications 6 (2015) 1..
[9] C. Huang, A. Narayan, E. Zhang, Y. Liu, X. Yan, J. Wang, C. Zhang, W. Wang, T. Zhou, C. Yi, *et al*., ACS nano 12 (2018) 7185.
[10] V. Fatemi, S. Wu, Y. Cao, L. Bretheau, Q. D. Gibson, K. Watanabe, T. Taniguchi, R. J. Cava, and P. Jarillo-Herrero, Science 362 (2018) 926.
[11] E. Sajadi, T. Palomaki, Z. Fei, W. Zhao, P. Bement,C. Olsen, S. Luescher, X. Xu, J. A. Folk, and D. H. Cobden, Science 362 (2018) 922.
[12] P. Giannozzi, S. Baroni, N. Bonini, M. Calandra, R. Car, C. Cavazzoni, D. Ceresoli, G. L. Chiarotti, M. Cococcioni, and I. Dabo *et al*., J. Phys. Condens. Matter 21 (2009) 395502.
[13] P. Giannozzi, O. Andreussi, T. Brumme, O. Bunau, M. B. Nardelli, M. Calandra, R. Car, C. Cavazzoni, D. Ceresoli, and M. Cococcioni *et al*., J. Phys. Condens. Matter 29 (2017) 465901.
[14] P. Giannozzi, O. Baseggio, P. Bonf, D. Brunato, R. Car, I. Carnimeo, C. Cavazzoni, S. de Gironcoli, P. Delugas, and F. Ferrari Ru no et al., J. Chem. Phys. 152 (2020) 154105.
[15] J. P. Perdew, K. Burke, and M. Ernzerhof, Phys. Rev. Lett. 77 (1996) 3865.
[16] B. G. Pfrommer, M. Côté S. G. Louie, and M. L. Cohen, J. Comp. Phys. 131 (1997) 233.
[17] H. J. Monkhorst and J. D. Pack, Phys. Rev. B, 13 (1976) 5188.
[18] N. Marzari, D. Vanderbilt, A. De Vita, and M. Payne, Phys. Rev. Lett. 82 (1999) 3296.
[19] E. Torun, H. Sahin, S. Cahangirov, A. Rubio, andF. Peeters, Journal of Applied Physics 119, (2016) 074307.
[20] Y.-j. Liu, B. Gao, D. Xu, H.-m. Wang, and J.-X. Zhao, Phys. Lett. A 378 (2014) 2989.
[21] W. Ku, T. Berlijn, C.-C. Lee, *et al.*, Physical review letters 104 (2010) 216401.